Spectra and flow of light nuclei in relativistic heavy ion collisions at energies available at the BNL Relativistic Heavy Ion Collider and at the CERN Large Hadron Collider

Wenbin Zhao, Lilin Zhu, Hua Zheng, Che Ming Ko, and Huichao Song

Phys. Rev. C **98**, 054905 — Published 21 November 2018

DOI: 10.1103/PhysRevC.98.054905

Spectra and flow of light nuclei in relativistic heavy ion collisions at energies available at the BNL Relativistic Heavy Ion Collider and at the CERN Large Hadron Collider

Wenbin Zhao,[1,2] Lilin Zhu,[3] Hua Zheng,[4,5] Che Ming Ko,[6] and Huichao Song[1,2,7]

[1]*Department of Physics and State Key Laboratory of Nuclear Physics and Technology, Peking University, Beijing 100871, China*
[2]*Collaborative Innovation Center of Quantum Matter, Beijing 100871, China*
[3]*Department of Physics, Sichuan University, Chengdu 610064, China*
[4]*School of Physics and Information Technology, Shaanxi Normal University, Xi'an 710119, China*
[5]*Laboratori Nazionali del Sud, INFN, via Santa Sofia, 62, 95123 Catania, Italy*
[6]*Cyclotron Institute and Department of Physics and Astronomy, Texas A&M University, College Station, TX 77843, USA*
[7]*Center for High Energy Physics, Peking University, Beijing 100871, China*

(Dated: November 5, 2018)

Within the framework of the coalescence model based on the phase-space distributions of protons and neutrons generated from the `iEBE-VISHNU` hybrid model with `AMPT` initial conditions, we study the spectra and elliptic flow of deuterons and helium-3 in relativistic heavy ion collisions at the Relativistic Heavy Ion Collider (RHIC) and the Larger Hadron Collider (LHC). Results from our model calculations for Au + Au collisions at $\sqrt{s_{NN}} = 200$ GeV at RHIC and Pb+Pb collisions at $\sqrt{s_{NN}} = 2.76$ TeV at the LHC are compared with available experimental data. Good agreements are generally seen between theoretical results and experimental data, except that the calculated yield of helium-3 in Pb + Pb collisions at $\sqrt{s_{NN}} = 2.76$ TeV underestimates the data by about a factor of two. Possible reasons for these discrepancies are discussed. We also make predictions on the spectra and elliptic flow of deuterons and helium-3 in Pb + Pb collisions at $\sqrt{s_{NN}} = 5.02$ TeV that are being studied at LHC.

PACS numbers: 25.75.Ld, 25.75.Gz, 24.10.Nz

I. INTRODUCTION

The production of light nuclei and their antiparticles in relativistic heavy ion collisions is a topic of great interest as it provides a unique opportunity to investigate whether nuclei and antinuclei have the same properties and to discover if exotic antinuclei can exist in nature [1–4]. Recently, the production of light nuclei has been widely measured at RHIC at BNL [2, 5–7] and the LHC at CERN [4, 8, 9]. The related theoretical investigations have been carried out in the frameworks of either the statistical model or the coalescence model. In the statistical model, the yields of hadrons and light nuclei can be nicely described with a few parameters related to the chemical freeze-out conditions [10, 11]. In the coalescence model, light nuclei are formed through the recombination of protons and neutrons with close positions and velocities on the kinetic freeze-out surface [12–20].

Although both the statistical model and the coalescence model can describe the yields of light nuclei at RHIC and LHC, it is generally believed that light nuclei formed from the statistical hadronization at chemical freeze-out can hardly remain stable during the hadronic evolution due to their small binding energies. Recently, the STAR, PHENIX and ALICE Collaborations have further measured the elliptic flow of deuterons (d) and helium-3 (^{3}He) in Au+Au collisions at $\sqrt{s_{NN}} = 200$ GeV [1, 21–23] and in Pb+Pb collisions at $\sqrt{s_{NN}} = 2.76$ TeV [4, 9]. It was found that the elliptic flow of these two light nuclei could not be described with the blast-wave model through simply replacing the proton mass with the ones of the light nuclei [23]. Also, the simplest or naive coalescence model [24], which assumes that the deuteron elliptic flow at certain transverse momentum is twice of that of the proton at half of the transverse momentum [9], failed to reproduce the measured elliptic flow of deuterons. On the other hand, Refs. [18, 19] showed that the spectra and elliptic flow of light nuclei could be described by the coalescence model using the phase-space distribution of nucleons generated from a modified blast-wave model. Besides the usual parameters, such as the fugacity ξ, the kinetic freeze-out temperature T_K, the nucleon emission proper time τ_0, the radial flow velocity $\beta(r)$ and p_T-dependent elliptic flow harmonic coefficient $\varepsilon(p_T)$, etc., which are required to fit the spectra and elliptic flow of pions, kaons and protons, additional space-momentum correlations between protons and neutrons are required in this study to fit the elliptic flow of deuterons and helium-3.

These previous studies [18, 19] have revealed that the formation of light nuclei is very sensitive to the phase-space distributions of protons and neutrons at kinetic freeze-out, which are strongly influenced by the dynamical evolution of the QGP and the hadronic fireball. In the standard model of relativistic heavy ion collisions, the evolving system after thermalization is described by hydrodynamics for the QGP fluid followed by a hadron cascade simulations for the hadronic evolution [25–31]. One such standard model is the `iEBE-VISHNU` hybrid model [31] that combines the (2+1)-d viscous hydrodynamics [32, 33] with the UrQMD hadron cascade model [34, 35]. During the past few years, `iEBE-VISHNU`

has been widely used to study various soft physics at RHIC and LHC, and this has led to many nice descriptions and predictions of various flow data, including flow harmonics, flow distributions, symmetric cumulants, event plane correlations, etc. [27, 36–42]. In particular, the iEBE-VISHNU hybrid model with AMPT initial conditions has successfully described and predicted the spectra and flow harmonics of pions, kaons and protons in Pb+Pb collisions at $\sqrt{s_{NN}} = 2.76$ and 5.02 TeV [36, 38, 43, 44]. The iEBE-VISHNU+UrQMD model with AMPT initial conditions is thus expected to provide the realistic phase-space distributions of protons and neutrons that are needed for the coalescence calculations of light nuclei production in relativistic heavy ion collisions. In this paper, we will use the nucleon phase-space distributions from this model to study and predict the spectra and elliptic flow of deuterons and helium-3 in Au+Au collisions at $\sqrt{s_{NN}} = 200$ GeV and in Pb+Pb collisions at $\sqrt{s_{NN}} = 2.76$ and 5.02 TeV in the framework of coalescence model. We emphasize that the parameters in iEBE-VISHNU simulations have been fixed by the yields, spectra and flow harmonics of all charged hadrons in previous studies [36, 38]. Compared with the modified blast-wave model [18, 19] that introduces a parametrized space-momentum correlation of nucleons to describe the elliptic flow of light nuclei, such space-momentum correlations of emitted hadrons are naturally included in iEBE-VISHNU through the dynamically generated nucleon distribution function without additional free parameters [25].

This paper is organized as the following: Sec. II and Sec III briefly introduce the coalescence model, the iEBE-VISHNU hybrid model and the set-ups of the calculations. Sec. IV presents and discusses the spectra and elliptic flow of deuterons and helium-3 in Au+Au collisions at $\sqrt{s_{NN}} = 200$ GeV and Pb+Pb collisions at $\sqrt{s_{NN}} = 2.76$ and 5.02 TeV, calculated with the coalescence model using phase-space distributions of nucleons from VISHNU. Sec. V summarizes the results and gives the conclusion from the present study.

II. THE COALESCENCE MODEL

In the coalescence model [45–47], the production probability of a nucleus of atomic number A is given by the overlap of the Wigner function $f_A(\mathbf{x}'_1, ..., \mathbf{x}'_A; \mathbf{p}'_1, ..., \mathbf{p}'_A, t')$ of the nucleus with the phase-space distributions $f(\mathbf{x}_i, \mathbf{p}_i, t)$ of nucleons at the kinetic freeze-out:

$$\frac{d^3N_A}{d\mathbf{P}_A^3} = g_A \int \Pi_{i=1}^A p_i^\mu d^3\sigma_{i\mu} \frac{d^3\mathbf{p}_i}{E_i} f(\mathbf{x}_i, \mathbf{p}_i, t) \times f_A(\mathbf{x}'_1, ..., \mathbf{x}'_A; \mathbf{p}'_1, ..., \mathbf{p}'_A; t') \delta^{(3)}\left(\mathbf{P}_A - \sum_{i=1}^A \mathbf{p}_i\right), \quad (1)$$

where $g_A = (2J_A + 1)/[\Pi_{i=1}^A (2J_i + 1)]$ is the statistical factor for A nucleons of spins J_i to form a nucleus of angular momentum J_A. The coordinate and momentum of the i-th nucleon in the fireball frame are denoted by $\mathbf{x}_i$ and $\mathbf{p}_i$, respectively. Their coordinate $\mathbf{x}'_i$ and momentum $\mathbf{p}'_i$ in the Wigner function of the produced nucleus are obtained by Lorentz transforming the coordinate $\mathbf{x}_i$ and momentum $\mathbf{p}_i$ to the rest frame of the nucleus and then propagating earlier freeze-out nucleons freely with a constant velocity, determined by the ratio of its momentum and energy in the rest frame of the nucleus, to the time t' when the last constituent nucleon in the nucleus freezes out.

In this paper, we focus on investigating deuteron and helium-3 production and elliptic flow. Following Ref. [47], their corresponding Wigner functions are obtained from the Wigner transformation of their wave functions, which are taken to be the product of the harmonic oscillator wave functions. In this case, the Wigner function of deuteron is [48]

$$f_2(\boldsymbol{\rho}, \mathbf{p}_\rho) = 8 \exp\left[-\frac{\boldsymbol{\rho}^2}{\sigma_\rho^2} - \mathbf{p}_\rho^2 \sigma_\rho^2\right], \quad (2)$$

where the relative coordinate $\boldsymbol{\rho}$ and relative momentum $\mathbf{p}_\rho$ are defined as:

$$\boldsymbol{\rho} = \frac{1}{\sqrt{2}}(\mathbf{x}'_1 - \mathbf{x}'_2), \quad \mathbf{p}_\rho = \sqrt{2}\,\frac{m_2\mathbf{p}'_1 - m_1\mathbf{p}'_2}{m_1 + m_2}, \quad (3)$$

with m_i being the mass of nucleon i. The width parameter σ_ρ in Eq. (2) is related to the root-mean-square radius of deuteron via [48]

$$\langle r_d^2 \rangle = \frac{3}{2}\frac{m_1^2 + m_2^2}{(m_1 + m_2)^2}\sigma_\rho^2 = \frac{3}{4}\frac{m_1^2 + m_2^2}{\omega m_1 m_2 (m_1 + m_2)}, \quad (4)$$

if we use the relation $\sigma_\rho = 1/\sqrt{\mu_1\omega}$ in terms of the oscillator frequency ω in the harmonic wave function and the reduced mass $\mu_1 = 2(1/m_1 + 1/m_2)^{-1}$.

Similarly, the Wigner function of helium-3 is [48]

$$f_3(\boldsymbol{\rho}, \boldsymbol{\lambda}, \mathbf{p}_\rho, \mathbf{p}_\lambda) = 8^2 \exp\left[-\frac{\boldsymbol{\rho}^2}{\sigma_\rho^2} - \frac{\boldsymbol{\lambda}^2}{\sigma_\lambda^2} - \mathbf{p}_\rho^2\sigma_\rho^2 - \mathbf{p}_\lambda^2\sigma_\lambda^2\right], \quad (5)$$

where $\boldsymbol{\rho}$ and $\mathbf{p}_\rho$ are similarly defined as in Eq. (3), and the relative coordinate $\boldsymbol{\lambda}$ and momentum $\mathbf{p}_\lambda$ are defined as:

$$\boldsymbol{\lambda} = \sqrt{\frac{2}{3}}\left(\frac{m_1\mathbf{x}'_1 + m_2\mathbf{x}'_2}{m_1 + m_2} - \mathbf{x}'_3\right), \quad \mathbf{p}_\lambda = \sqrt{\frac{3}{2}}\,\frac{m_3(\mathbf{p}'_1 + \mathbf{p}'_2) - (m_1 + m_2)\mathbf{p}'_3}{m_1 + m_2 + m_3}. \quad (6)$$

The width parameter σ_λ in Eq.(5) is related to the oscillator frequency by $\sigma_\lambda = 1/\sqrt{\mu_2\omega}$ with $\mu_2 = (3/2)[1/(m_1 + m_2) + 1/m_3]^{-1}$. The values of σ_ρ and σ_λ are determined

from the oscillator constant via the root-mean-square radius of helium-3 by [48]

$$\langle r_{He}^2\rangle = \frac{1}{2}\frac{m_1^2(m_2+m_3)+m_2^2(m_3+m_1)+m_3^2(m_1+m_2)}{\omega(m_1+m_2+m_3)m_1m_2m_3}. \quad (7)$$

For the production of helium-3, besides the coalescence process $p+p+n \to {}^3$He from two protons and one neutron, we also include the coalescence process $d+p \to {}^3$He from one deuteron and one proton. Here, the deuteron is treated as a point particle with its phase-space distribution given by that obtained from the coalescence of proton and neutron, the corresponding two-body Wigner function of helium-3 is given by Eq. (2) with $\boldsymbol{\rho}$ and $\mathbf{p}_\rho$ denoting the relative coordinate and momentum between deuteron and proton.

TABLE I: Statistical factor (g), radius (R), oscillator frequency (ω), and width parameters (σ_ρ, σ_λ) for deuteron and helium-3. Radii are taken from Ref. [49].

Nucleus	g	R (fm)	ω (sec^{-1})	$\sigma_\rho, \sigma_\lambda$ (fm)
deuteron	3/4	2.1421	0.1739	2.473
$p+p+n \to {}^3$He	1/4	1.9661	0.5504	1.390
$d+p \to {}^3$He	1/3	1.9661	0.3389	1.536

The statistical factors and values of the width parameters in the Wigner functions for deuteron and helium-3 as well as the empirical values of their charge radii and resulting oscillator constants are given in TABLE I. We note that as in most studies on application of the coalescence model for deuteron production , the statistical factors given in TABLE I do not include that due to isospin, which would reduce the value for $p+n \to d$ by a factor of 2 and the value for $p+p+n \to {}^3$He by a factor of 3 [45, 50, 51]. Since whether to include isospin in determining the statistical factors in the coalescence model is still an unresolved question, we give in Appendix A our arguments for not including this in our consideration.

III. THE iEBE-VISHNU HYBRID MODEL

In this paper, we use the iEBE-VISHNU hybrid model to generate the phase-space distributions of nucleons for the coalescence model calculations of light nuclei. The iEBE-VISHNU model [31] is an event-by-event version of the VISHNU hybrid model [25] that combines the (2+1)-d viscous hydrodynamics VISH2+1 [32, 33] for the QGP expansion with the hadron cascade model UrQMD [34, 35] for the evolution of subsequent hadronic matter. In the present study, we follow Refs. [36, 38] to set the starting time of hydrodynamics at $\tau_0 = 0.6$ fm/c and implement the AMPT initial conditions to generate the fluctuating initial profiles of energy density in the transverse plane with zero transverse velocity. Also, the normalization factors for the initial energy density profiles are tuned to fit the yields of all charged hadrons in Au + Au collisions at $\sqrt{s_{NN}} = 200$ GeV or in Pb + Pb collisions at $\sqrt{s_{NN}} = 2.76$ and 5.02 TeV. In iEBE-VISHNU, the transport equations for energy-momentum tensor $T^{\mu\nu}$ and the 2nd order Israel-Stewart equations for shear stress tensor $\pi^{\mu\nu}$ and bulk pressure Π for the QGP evolution are solved by using the (2+1)-d viscous hydrodynamics VISH2+1 with longitudinal boost invariance [32, 33, 52]. Following Refs. [36, 38], we set the specific shear viscosity and specific bulk viscosity in QGP to $\eta/s = 0.08$ and $\zeta/s = 0$, respectively, and use the equation of state from the HotQCD Collaboration [53, 54]. The switching temperature T_{sw} that controls the transition from the hydrodynamic evolution to the hadron cascade simulation is set to 148 MeV. After the UrQMD hadronic evolution, we output the coordinate and momentum information of various stable hadrons at the kinetic freeze-out, which can be used to calculate the spectra and flow observables as well as to provide the phase-space distributions of nucleons for the coalescence model study of light nuclei production.

We emphasize that with the above set-ups and the fine tuned parameters in AMPT initial conditions [36, 38], iEBE-VISHNU could nicely describe various soft hadron data at RHIC and LHC, especially on the p_T spectra and flow harmonics of pions, kaons and protons [36, 38]. This indicates that iEBE-VISHNU can generate proper phase-space distributions of nucleons at the kinetic freeze-out for the coalescence model calculations. Compared with previous studies based on the blast-wave model [18, 19], the space-momentum correlations of nucleons are naturally included in iEBE-VISHNU through the dynamically generated distribution functions without introducing any free parameters [25]. Details of parameter fitting and results on the spectra and various flow data of all charged and identified hadrons within the framework of iEBE-VISHNU can be found in Refs. [36, 38].

IV. RESULTS

Using the phase-space distributions of protons and neutrons from the iEBE-VISHNU hybrid model with AMPT initial conditions as described in Section III, we show in the following the transverse momentum spectra and elliptic flow of deuterons and helium-3 in Au + Au collisions at $\sqrt{s_{NN}} = 200$ GeV and in Pb + Pb collisions at $\sqrt{s_{NN}} = 2.76$ and 5.02 TeV obtained from the coalescence model described in Section II.

A. Au + Au collisions at $\sqrt{s_{NN}} = 200$ GeV

Figure 1 shows the transverse momentum spectra of protons, deuterons and helium-3 in Au + Au collisions at $\sqrt{s_{NN}} = 200$ GeV and 0-80% centrality. The spectrum of protons is calculated from the iEBE-VISHNU hy-

brid model with AMPT initial conditions , which nicely describes the PHENIX data below 3 GeV. With the phase-space distributions of protons and neutrons from iEBE-VISHNU, we calculate the spectra of deuterons and helium-3 using the coalescence model. As shown by the blue dotted line in Fig. 1, our model calculation nicely reproduces the deuteron data from PHENIX [21]. For the transverse momentum spectrum of helium-3, our calculations that include the two coalescence processes $p+p+n \rightarrow {}^3\mathrm{He}$ and $p+d \rightarrow {}^3\mathrm{He}$ roughly describe the data from STAR, while including only the single coalescence process $p+p+n \rightarrow {}^3\mathrm{He}$ significantly under-predicts the data for helium-3 as described in details in the Appendix. We thus include in the present study both coalescence processes to calculate the spectrum and elliptic flow of helium-3 as in Ref. [55].

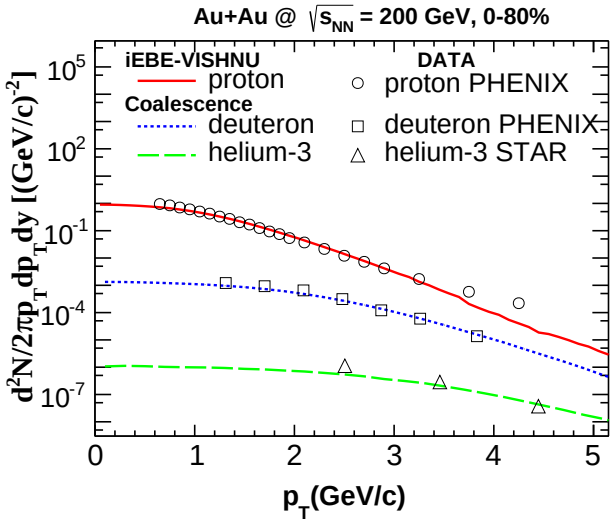

FIG. 1: Transverse momentum spectra of protons, deuterons and helium-3 in Au + Au collisions at $\sqrt{s_{NN}} = 200$ GeV and 0-80% centrality, calculated from the iEBE-VISHNU hybrid model (protons) and from the coalescence model (deuterons and helium-3) using the phase-space distributions of protons and neutrons from iEBE-VISHNU. The data for protons, deuterons and helium-3 are taken from the PHENIX [21, 56] and STAR [1] Collaborations, respectively.

Figure 2 shows the differential elliptic flow $v_2(p_T)$ of protons, deuterons and helium-3 in Au + Au collisions at $\sqrt{s_{NN}} = 200$ GeV and 0-80% centrality. Following Refs. [22, 23], we calculate $v_2(p_T)$ using the event-plane method with particle of interest (POIs) and reference particles (RPs) selected from two sub-events with their pseudorapidity η taken within $-1.0 < \eta < 0$ and $0 < \eta < 1.0$, respectively. It is seen that the iEBE-VISHNU hybrid model with AMPT initial conditions and other tuned parameters [38, 39] gives an overall quantitative description of $v_2(p_T)$ of protons below 2.5 GeV but becomes increasingly larger than the data as the proton momentum increases, where the hydrodynamic approach becomes not applicable. The elliptic flow of deuterons and helium-3 from the coalescence model using the phase-space distributions of protons and neutrons from iEBE-VISHNU can roughly describe the measured data from the STAR Collaboration, including the clear v_2 mass ordering among protons, deuterons and helium-3. On the other hand, the measured and calculated elliptic flow of deuterons gradually deviate from each other above 2 GeV in Au+Au collisions at $\sqrt{s_{NN}} = 200$ GeV, which is surprising as one would expect a well-tuned phase-space distributions of protons below 2 GeV be able to describe the elliptic flow of deuterons up to a momentum of 4 GeV. This discrepancy between the model result and data from 2 to 4 GeV for deuterons at RHIC requires further study.

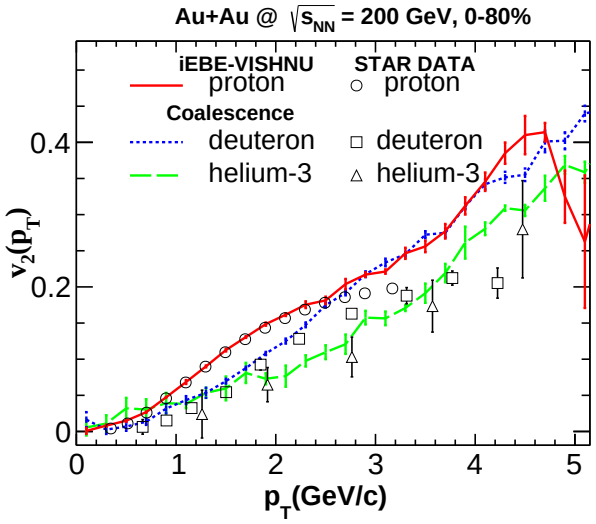

FIG. 2: Elliptic flow of protons, deuterons and helium-3 in Au + Au collisions at $\sqrt{s_{NN}} = 200$ GeV and 0-80% centrality, calculated from iEBE-VISHNU (protons) and from the coalescence model (deuterons and helium-3). The data of protons, deuterons and helium-3 are taken from the STAR Collaboration [22, 23].

B. Pb + Pb collisions at $\sqrt{s_{NN}} = 2.76$ and 5.02 TeV

Figure 3 shows the transverse momentum spectra of protons, deuterons and helium-3 in Pb + Pb collisions at $\sqrt{s_{NN}} = 2.76$ and 5.02 TeV. Similar to Fig. 1 for Au+Au collisions at $\sqrt{s_{NN}} = 200$ GeV, the spectra of protons shown in the left panel of Fig. 3 are calculated from iEBE-VISHNU with AMPT initial conditions nicely describes the ALICE data below 3 GeV in Pb+Pb collisions at $\sqrt{s_{NN}} = 2.76$ TeV for various centralities. With retuned parameters that fit the measured multiplicity [39], we predict the spectra of protons in Pb + Pb collisions at $\sqrt{s_{NN}} = 5.02$ TeV with iEBE-VISHNU, which are seen to be higher and flatter than the ones at $\sqrt{s_{NN}} = 2.76$ TeV due to larger multiplicity and stronger radial flow [36]. The spectra of deuterons obtained with the coalescence model using the phase-space distributions of protons and neutrons from iEBE-VISHNU are shown in the middle

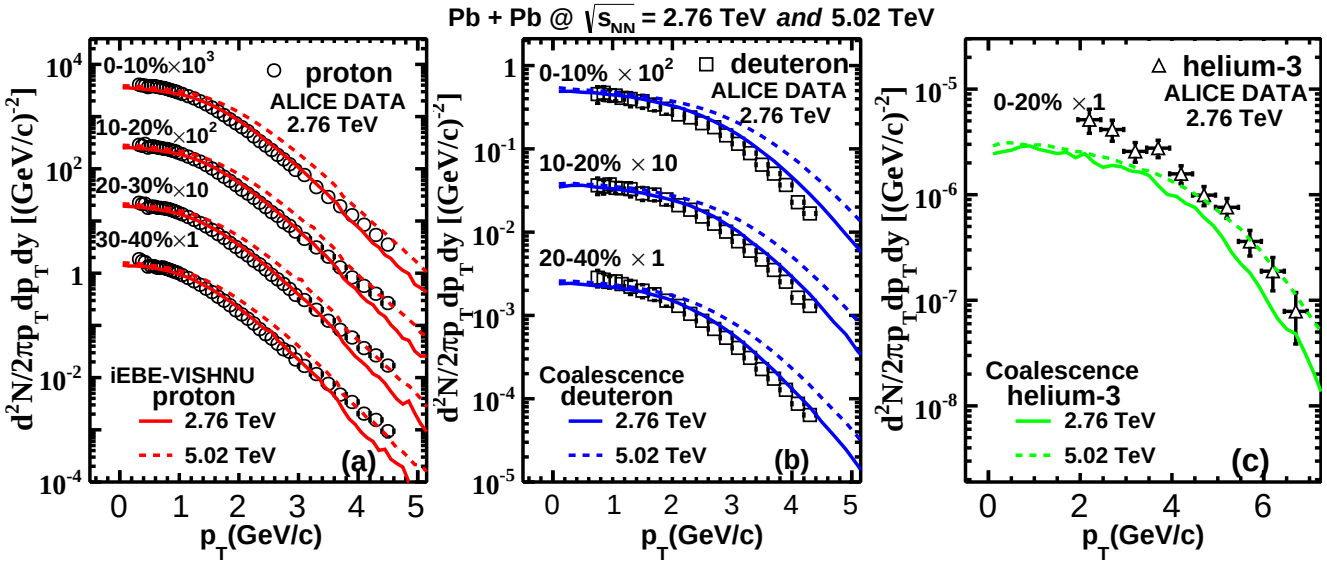

FIG. 3: Transverse momentum spectra of protons, deuterons and helium-3 in Pb + Pb collisions at $\sqrt{s_{NN}}$ = 2.76 and 5.02 TeV, calculated from iEBE-VISHNU (protons) and from the coalescence model (deuterons and helium-3). The data for protons, deuterons and helium-3 at $\sqrt{s_{NN}}$ = 2.76 and 5.02 TeV are taken from Refs. [9, 57] and [4], respectively.

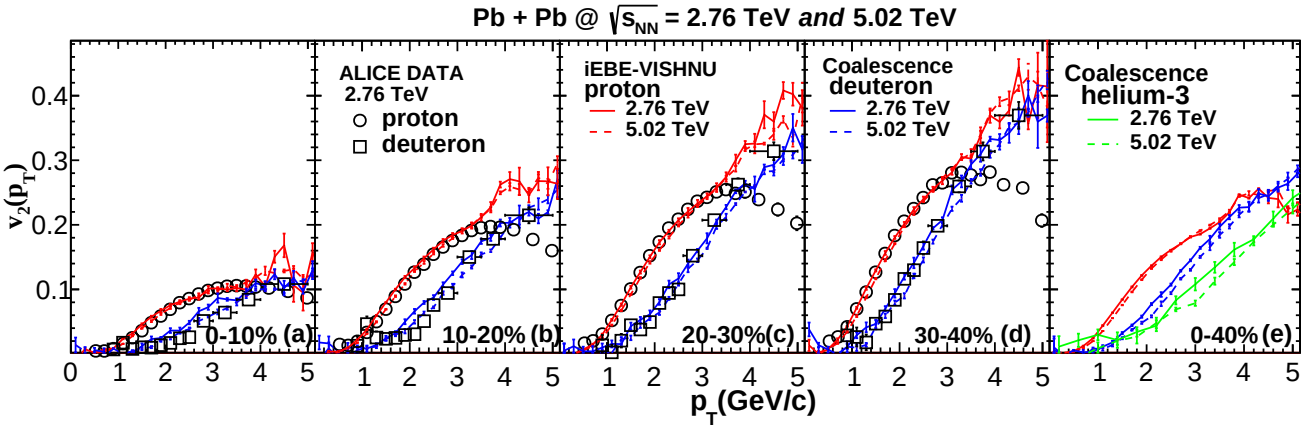

FIG. 4: Elliptic flow of protons, deuterons and helium-3 in Pb + Pb collisions at $\sqrt{s_{NN}}$ = 2.76 and 5.02 TeV, calculated from iEBE-VISHNU (protons) and from the coalescence model (deuterons and helium-3). The data for protons and deuterons at $\sqrt{s_{NN}}$ = 2.76 TeV are taken from Refs. [43] and [9], respectively.

panel of Fig. 3. Our calculations are seen to describe the low-p_T spectra of deuterons from ALICE for Pb + Pb collisions at $\sqrt{s_{NN}}$ = 2.76 TeV and 0-10%, 10-20% and 20-40% centralities, but to slightly over-predict the data above 2.5 GeV for these three centralities. We also predict the transverse momentum spectra of deuterons in Pb + Pb collisions at $\sqrt{s_{NN}}$ = 5.02 TeV, which are higher and flatter than the ones at $\sqrt{s_{NN}}$ = 2.76 TeV as the case for protons. The right panel of Fig. 3 shows the transverse momentum spectrum of helium-3 in Pb +Pb collisions at $\sqrt{s_{NN}}$ = 2.76 and 5.02 TeV for 0-20% centrality that are calculated and predicted from the coalescence model respectively. As in the calculations for Au+Au collisions at $\sqrt{s_{NN}}$ = 200 GeV, we include both coalescence processes $p + p + n \rightarrow {}^3$He and $d + p \rightarrow {}^3$He, which approximately double the yield of helium-3 for the case of the single coalescence process $p + p + n \rightarrow {}^3$He. However, the yield of helium-3 in Pb +Pb collisions at $\sqrt{s_{NN}}$ = 2.76 TeV is still largely underestimated, which also leads to an under-prediction of its spectrum. Detailed discussions on this are given in Appendix B.

Figure 4 shows the elliptic flow of protons, deuterons and helium-3 in Pb + Pb collisions at $\sqrt{s_{NN}}$ = 2.76 and 5.02 TeV. Following Refs. [9, 43], we use the Q-cumulant method to calculate $v_2(p_T)$ for protons and deuterons. Shown in the four panels to the left of Fig. 4 are the results at $0-10\%$, $10-20\%$, $20-30\%$, and $30-40\%$ centralities, respectively. Results from our calculations give a nice description of the measured $v_2(p_T)$ of protons up to 3 GeV at these centralities in Pb + Pb collisions

at $\sqrt{s_{NN}} = 2.76$ TeV [44]. The red dashed lines are predicted $v_2(p_T)$ of protons at 5.02 TeV, which are slightly lower than the ones at 2.76 TeV due to the slightly increased radial flow at larger collision energy, and this is consistent with recent ALICE experimental data [44]. For the deuteron elliptic flow in collisions at 20-30% and 30-40% centralities, our model calculations based on the coalescence model using the phase-space distributions of protons and neutrons from `iEBE-VISHNU` can quantitatively describe its momentum dependence up to 4 GeV within error bars. However, for collisions at $0-10\%$ and $10-20\%$ centralities, our model calculations slightly over-predict the data above 1.5 GeV, although the input phase-space distribution of protons describes the corresponding $v_2(p_T)$ of protons well. The predicted elliptic flow of deuterons at $\sqrt{s_{NN}}$= 5.02 TeV are slightly below the one at 2.76 TeV, which is similar to the case of protons.

Due to limited statistics, we only calculate the elliptic flow of helium-3 at $0-40\%$ centrality as shown in the right panel of Fig. 4. As in recent experimental measurements [58], we use the Event Plane (EP) method with two sub-events within $-1.0 < \eta < 0$ and $0 < \eta < 1.0$ to calculate the $v_2(p_T)$ of protons, deuterons and helium-3 at this centrality instead of the Q-cumulant method used for other centralities. Results from our model calculations show a clear v_2 mass ordering among protons, deuterons and helium-3. With increasing collision energies, the difference between protons and helium-3 v_2 also increases. Such v_2 mass ordering is similar to that in Au+Au collisions at $\sqrt{s_{NN}} = 200$ GeV, which can also be tested in future experiments.

V. SUMMARY

In this paper, we have studied the spectra and elliptic flow of deuterons and helium-3 in relativistic heavy ion collisions at RHIC and LHC in the coalescence model. The needed phase-space distributions of protons and neutrons at kinetic freeze-out are generated from the `iEBE-VISHNU` hybrid model with `AMPT` initial conditions, which have been shown to describe nicely the spectra and elliptic flow of pions, kaons and protons in previous calculations [36, 38]. Results from our coalescence model calculations are found to roughly describe the p_T spectra of deuterons and the differential elliptic flow of deuterons and helium-3 at various centralities in Au + Au collisions at $\sqrt{s_{NN}} = 200$ GeV and in Pb + Pb collisions at $\sqrt{s_{NN}} = 2.76$ TeV. We have also predicted the spectra and elliptic flow of deuterons and helium-3 in Pb + Pb collisions at $\sqrt{s_{NN}} = 5.02$ TeV, which can be compared with experimental measurements in the near future. The agreement between our model calculations and available data at RHIC and LHC indicates that the coalescence model, together with the proper phase-space distributions of nucleons generated from a realistic hybrid model, supports the picture that light nuclei are produced through the coalescence of protons and neutrons in relativistic heavy ion collisions at RHIC and LHC.

Although the coalescence model nicely describes the elliptic flow of helium-3 at RHIC and the LHC, there exists a discrepancy between the calculated and measured p_T spectrum of helium-3 in Pb + Pb collisions at $\sqrt{s_{NN}} = 2.76$ TeV. Although including the two coalescence processes $p+p+n \to {}^3\mathrm{He}$ and $p+d \to {}^3\mathrm{He}$ in our coalescence model calculations can roughly describe the p_T spectra of helium-3 in Au + Au collisions at $\sqrt{s_{NN}} = 200$ GeV, it under-predicts the yield of helium-3 in Pb + Pb collisions at $\sqrt{s_{NN}} = 2.76$ TeV. The reason for this discrepancy may be due to its earlier formation than the deuteron in collisions at higher energies as discussed in the Appendix B.

Acknowledgements

We thank the discussions from K. Sun, H. Xu and J. Zhao. W. Z. and H. S. are supported by the NSFC and the MOST under grant Nos. 11435001, 11675004 and 2015CB856900. L. L. Z is supported in part by the NSFC of China under Grant no. 11205106. C. M. K is supported by the US Department of Energy under Contract No. DE-SC0015266 and the Welch Foundation under Grant No. A-1358. W. Z. and H. S. also gratefully acknowledge the extensive computing resources provided by the Super-computing Center of Chinese Academy of Science (SCCAS), Tianhe-1A from the National Supercomputing Center in Tianjin, China and the High-performance Computing Platform of Peking University.

Appendix A: Statistical factors in the coalescence model

In this Appendix, we give arguments for not considering isospin in determining the statistical factors in our application of the coalescence model to light nuclei production. Using deuteron production as an example, we first note that the coalescence model is based on the sudden approximation to evaluate the probability for deuteron production from proton and neutron interactions at kinetic freeze-out of a heavy ion collision. For collisions at relativistic energies with the final hadronic matter consisting mainly of pions, to conserve both momentum and energy, deuteron production actually takes place through the process $pn\pi \to d\pi$ with the extra π taking up the energy released from forming the bound deuteron [59]. Since the π has isospin one, its interaction with the proton-neutron pair has both isoscalar and isovector components. While the isoscalar interaction does not affect the isospin of the proton and neutron, which can be either one or zero with the latter to be able to form an isospin singlet deuteron, the isovector interaction can change the isospin one component of their wave function to isospin zero and then leads to the produc-

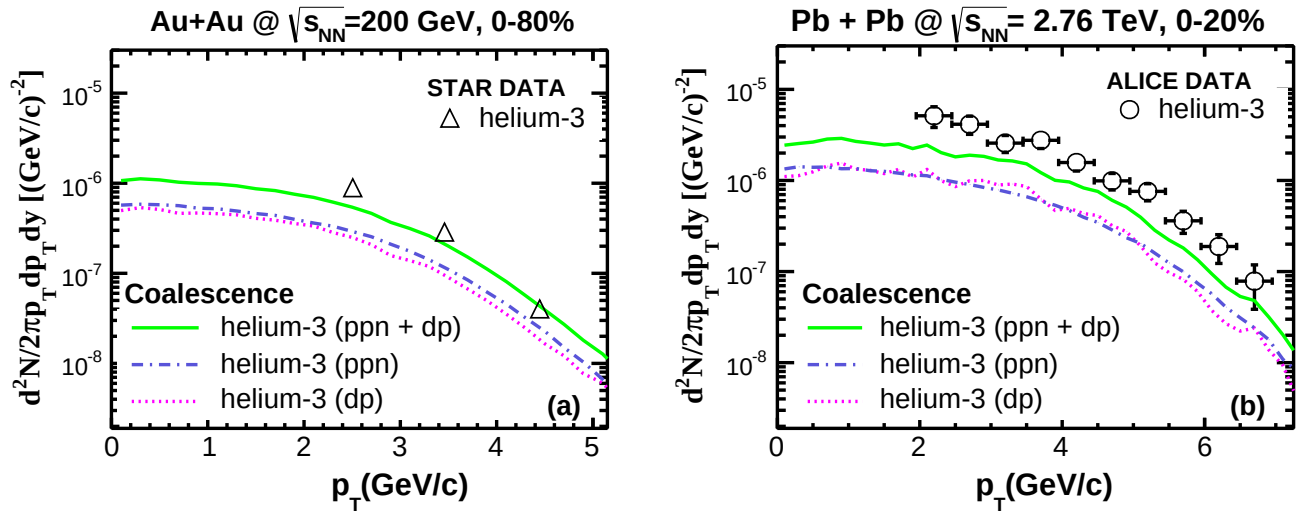

FIG. 5: Transverse momentum spectra of helium-3 in Au + Au collisions at $\sqrt{s_{NN}}$ = 200 GeV and 0-80% centrality and in Pb + Pb collisions at $\sqrt{s_{NN}}$ = 2.76 TeV and 0-20% centrality, calculated from the coalescence model using the phase-space distributions of protons and neutrons from `iEBE-VISHNU`. The blue dashed-dotted line and the pink dotted line are from the coalescence processes of $p+p+n \to {}^3$He and $p+d \to {}^3$He, respectively. The green solid line is the sum of these two processes. The data in Au + Au and Pb + Pb collisions are taken from the STAR Collaboration [1] and the ALICE Collaboration [4], respectively.

tion of a deuteron. Therefore, a proton and neutron pair can produce a deuteron even if they have total isospin one. Secondly, it has been shown in Ref. [60] that the coalescence model without considering isospin in the statistical factor gives the same deuteron yield as that from the thermal or statistical model if the binding energy and radius of deuteron are, respectively, much smaller than the temperature of the system and much larger than the thermal wavelength of the nucleons, which are generally satisfied in heavy ion collisions. That the deuteron can reach thermal and chemical equilibrium at kinetic freeze-out via the reactions $pn\pi \leftrightarrow d\pi$ during the hadronic stage of heavy ion collisions is not surprising if it exists at high temperature and density, which remains, however, to be verified due to its small binding energy. Indeed, studies based on both transport model [20] and kinetic approach [61] using the reactions $pn \leftrightarrow d\pi$ as the surrogate for the reactions $pn\pi \leftrightarrow d\pi$ have shown that the final deuteron yield is consistent with that from the coalescence model using protons and neutrons at kinetic freeze-out and the statistical factor without including isospin in the consideration.

Appendix B: Helium-3 production

In this appendix, we discuss in detail the production of helium-3 in relativistic heavy ion collisions at RHIC and LHC in the framework of the coalescence model that uses the phase-space distribution of kinetically freeze-out nucleons from the `iEBE-VISHNU` model with `AMPT` initial conditions. As briefly mentioned in Sec. IV, the yield of helium-3 measured in experiments cannot be reproduced by the coalescence model that includes only the coalescence process $p+p+n \to {}^3$He. A similar result has been found in a recent work on hypertriton production in relativistic heavy ion collisions [55]. In that study, the experimental data cannot be explained by the coalescence process $p+n+\Lambda \to {}^3_\Lambda$H alone. After also including the process $d+\Lambda \to {}^3_\Lambda$H, the yield of ${}^3_\Lambda$H is found to be enhanced by about a factor of two, which helps to achieve a better description of the experimental data. Following Ref. [55], we include in our study both processes $p+p+n \to {}^3$He and $d+p \to {}^3$He in the coalescence calculations of helium-3.

In Fig. 5, we show the p_T-spectra of helium-3 in Au + Au collisions at $\sqrt{s_{NN}}$ = 200 GeV and in Pb + Pb collisions at $\sqrt{s_{NN}}$ = 2.76 TeV, calculated from the coalescence model with $p+p+n \to {}^3$He (blue dashed-dotted line), with $d+p \to {}^3$He (pink dotted line) and with both these two processes (green solid line). At both RHIC and LHC collision energies, the spectra of helium-3 from the two coalescence processes $p+p+n \to {}^3$He and $p+d \to {}^3$He are close to each other. Adding the two contributions thus enhances the yield of helium-3 by about a factor of two, which roughly describes the measured p_T spectrum in Au+Au collisions. However, the calculated spectrum of helium-3 in Pb+Pb collisions from both coalescence processes still under-predicts the data.

In Ref. [20], deuteron production in Au + Au collisions at $\sqrt{s_{NN}}$ = 200 GeV has been studied within the transport approach by assuming that deuterons are initially statistically produced at chemical freeze-out and then followed by a hadronic evolution that includes both their annihilations and reproductions via the reactions $NN \leftrightarrow d\pi$. It is found that such transport approach gives a similar p_T spectrum of deuterons as the one obtained

from the coalescence model using the phase-space distributions of nucleons at kinetic freeze-out . This study thus indicates that for deuteron production at top RHIC energy, the coalescence model based on protons and neutrons at the kinetic freeze-out is a good approximation to the transport approach that takes into account their annihilations and reproductions. However, the production of helium-3 has not been investigated within the transport approach since it is highly nontrivial to include the three-particle interaction for helium-3 production from three nucleons. It is thus not clear whether the coalescence model for helium-3 production based on nucleons at kinetic freeze-out is also a good approximation to the transport model calculations. Also, it has been found in Ref. [41] that baryon-antibaryon annihilation is more significant in Pb + Pb collisions at $\sqrt{s_{NN}} = 2.76$ TeV than in Au + Au collisions at $\sqrt{s_{NN}} = 200$ GeV, due to the longer evolution time in the hadronic stage at higher collision energies, which may affect the time when helium-3 is produced from the coalescence of nucleons.

[1] B. I. Abelev *et al.* [STAR Collaboration], arXiv:0909.0566.
[2] H. Agakishiev *et al.* [STAR Collaboration], Nature **473**, 353 (2011).
[3] N. Sharma [ALICE Collaboration], J. Phys. G **38**, 124189 (2011).
[4] J. Adam *et al.* [ALICE Collaboration], Phys. Rev. C **93**, no. 2, 024917 (2016).
[5] N. Yu [STAR Collaboration], Nucl. Phys. A **967**, 788 (2017).
[6] C. Adler *et al.* [STAR Collaboration], Phys. Rev. Lett. **87**, 262301 (2001).
[7] B. I. Abelev *et al.* [STAR Collaboration], Science **328**, 58 (2010).
[8] J. Adam *et al.* [ALICE Collaboration], Phys. Lett. B **754**, 360 (2016).
[9] S. Acharya *et al.* [ALICE Collaboration], Eur. Phys. J. C **77**, no. 10, 658 (2017).
[10] A. Andronic, P. Braun-Munzinger, J. Stachel and H. Stocker, Phys. Lett. B **697**, 203 (2011).
[11] J. Cleymans, S. Kabana, I. Kraus, H. Oeschler, K. Redlich and N. Sharma, Phys. Rev. C **84**, 054916 (2011).
[12] G. Chen, Y. L. Yan, D. S. Li, D. M. Zhou, M. J. Wang, B. G. Dong and B. H. Sa, Phys. Rev. C **86**, 054910 (2012).
[13] G. Chen, H. Chen, J. Wu, D. S. Li and M. J. Wang, Phys. Rev. C **88**, no. 3, 034908 (2013).
[14] N. Shah, Y. G. Ma, J. H. Chen and S. Zhang, Phys. Lett. B **754**, 6 (2016).
[15] K. J. Sun and L. W. Chen, Phys. Lett. B **751**, 272 (2015).
[16] K. J. Sun and L. W. Chen, Phys. Rev. C **93**, no. 6, 064909 (2016).
[17] A. S. Botvina, J. Steinheimer and M. Bleicher, Phys. Rev. C **96**, no. 1, 014913 (2017).
[18] X. Yin, C. M. Ko, Y. Sun and L. Zhu, Phys. Rev. C **95**, no. 5, 054913 (2017).
[19] L. Zhu, H. Zheng, C. M. Ko and Y. Sun, Eur. Phys. J. A **54**, 175 (2018).
[20] Y. Oh, Z. W. Lin and C. M. Ko, Phys. Rev. C **80**, 064902 (2009).
[21] S. S. Adler *et al.* [PHENIX Collaboration], Phys. Rev. Lett. **94**, 122302 (2005).
[22] L. Adamczyk *et al.* [STAR Collaboration], Phys. Rev. Lett. **116**, no. 6, 062301 (2016).
[23] L. Adamczyk *et al.* [STAR Collaboration], Phys. Rev. C **94**, no. 3, 034908 (2016).
[24] P. F. Kolb, L. W. Chen, V. Greco and C. M. Ko, Phys. Rev. C **69**, 051901 (2004).
[25] H. Song, S. A. Bass and U. Heinz, Phys. Rev. C **83**, 024912 (2011).
[26] U. Heinz and R. Snellings, Ann. Rev. Nucl. Part. Sci. **63**, 123 (2013).
[27] H. Song, Y. Zhou and K. Gajdosova, Nucl. Sci. Tech. **28**, no. 7, 99 (2017).
[28] C. Gale, S. Jeon and B. Schenke, Int. J. Mod. Phys. A **28**, 1340011 (2013).
[29] H. Song, Pramana **84**, 703 (2015).
[30] B. Schenke, S. Jeon and C. Gale, Phys. Rev. Lett. **106**, 042301 (2011).
[31] C. Shen, Z. Qiu, H. Song, J. Bernhard, S. Bass and U. Heinz, Comput. Phys. Commun. **199**, 61 (2016).
[32] H. Song and U. W. Heinz, Phys. Lett. B **658**, 279 (2008).
[33] H. Song, Ph.D Thesis, The Ohio State University (August 2009), arXiv:0908.3656.
[34] S. A. Bass *et al.*, Prog. Part. Nucl. Phys. **41**, 255 (1998).
[35] M. Bleicher *et al.*, J. Phys. G **25**, 1859 (1999).
[36] W. Zhao, H. J. Xu and H. Song, Eur. Phys. J. C **77**, no. 9, 645 (2017).
[37] X. Zhu, Y. Zhou, H. Xu and H. Song, Phys. Rev. C **95**, no. 4, 044902 (2017).
[38] H. J. Xu, Z. Li and H. Song, Phys. Rev. C **93**, no. 6, 064905 (2016).
[39] W. Zhao, Y. Zhou, H. Xu, W. Deng and H. Song, Phys. Lett. B **780**, 495 (2018).
[40] J. Qian and U. Heinz, Phys. Rev. C **94**, no. 2, 024910 (2016).
[41] H. Song, S. Bass and U. W. Heinz, Phys. Rev. C **89**, no. 3, 034919 (2014).
[42] X. Zhu, F. Meng, H. Song and Y. X. Liu, Phys. Rev. C **91**, no. 3, 034904 (2015).
[43] J. Adam *et al.* [ALICE Collaboration], JHEP **1609**, 164 (2016).
[44] S. Acharya *et al.* [ALICE Collaboration], arXiv:1805.04390.
[45] R. Mattiello, H. Sorge, H. Stoecker and W. Greiner, Phys. Rev. C **55**, 1443 (1997).
[46] L. W. Chen, C. M. Ko and B. A. Li, Phys. Rev. C **68**, 017601 (2003).
[47] L. W. Chen, C. M. Ko and B. A. Li, Nucl. Phys. A **729**, 809 (2003).
[48] C. M. Ko, T. Song, F. Li, V. Greco and S. Plumari, Nucl. Phys. A **928**, 234 (2014).
[49] I. Angeli and K. P. Marinova, Atom. Data Nucl. Data Tabl. **99**, no. 1, 69 (2013).
[50] Y. Xia, J. Xu, B. A. Li and W. Q. Shen, Nucl. Phys. A **955**, 41 (2016).
[51] J. L. Nagle, B. S. Kumar, D. Kusnezov, H. Sorge and

R. Mattiello, Phys. Rev. C **53**, 367 (1996).
[52] H. Song and U. W. Heinz, Phys. Rev. C **77**, 064901 (2008).
[53] J. E. Bernhard, J. S. Moreland, S. A. Bass, J. Liu and U. Heinz, Phys. Rev. C **94** no.2, 024907 (2016).
[54] J. S. Moreland and R. A. Soltz, Phys. Rev. C **93**, no. 4, 044913 (2016).
[55] Z. Zhang and C. M. Ko, Phys. Lett. B **780**, 191 (2018).
[56] S. S. Adler *et al.* [PHENIX Collaboration], Phys. Rev. C **69**, 034909 (2004).
[57] B. Abelev *et al.* [ALICE Collaboration], Phys. Rev. C **88**, 044910 (2013).
[58] Maximiliano Puccio, presented at Quark Matter 2018 (unpublished).
[59] Y. Oh and C. M. Ko, Phys. Rev. C **76**, 054910 (2007).
[60] J. I. Kapusta, Phys. Rev. C **21**, 1301 (1980).
[61] S. Cho, T. Song and S. H. Lee, Phys. Rev. C **97**, no. 2, 024911 (2018).